

Electronic Supplementary Information

Albumin-mediated Platinum Nanocrystals for In Vivo Enhanced Computed Tomography Imaging

Zhiming Wang^{‡a}, Lina Chen^{‡b}, Chusen Huang^a, Yuankui Huang^b and Nengqin Jia^{a*}

^a The Education Ministry Key Laboratory of Resource Chemistry, Shanghai Key Laboratory of Rare Earth Functional Materials and Shanghai Municipal Education Committee Key Laboratory of Molecular Imaging Probes and Sensors, Department of Chemistry, Shanghai Normal University, Shanghai 200234, People's Republic of China

^b Jingzhou Central Hospital, The Second Clinical Medical College, Yangtze University, Jingzhou 434020, People's Republic of China

* Corresponding author: Nengqin Jia

E-mail: nqjia@shnu.edu.cn.

Tel: +86-21-64321045

Fax: +86-21-64321833

‡ These authors equally contributed to this work.

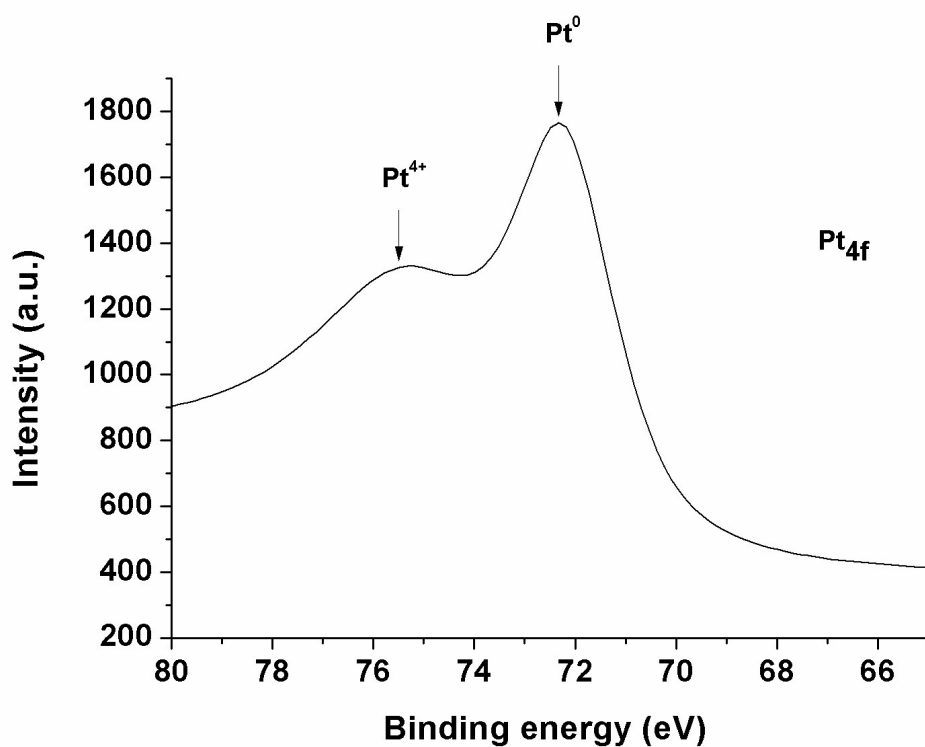


Fig. S1 Normalized Pt 4f XPS spectra of Pt@BSA nanocrystals.

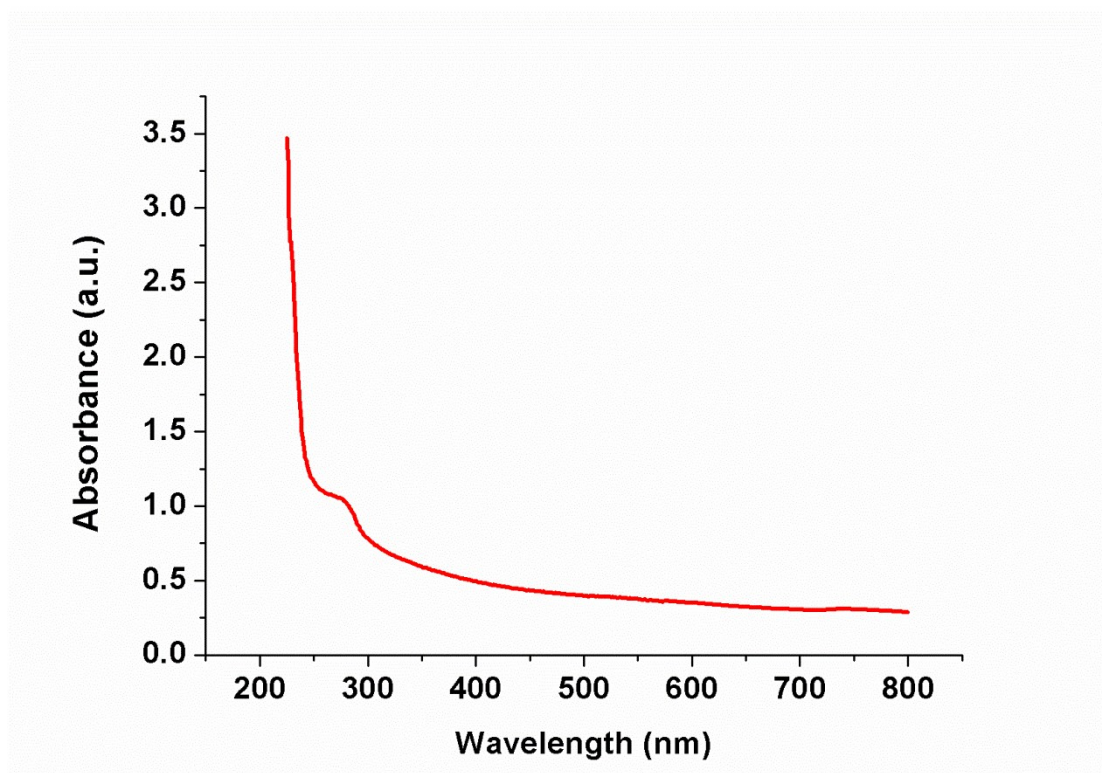


Fig. S2 UV-Vis spectra of Pt@BSA nanocrystals.

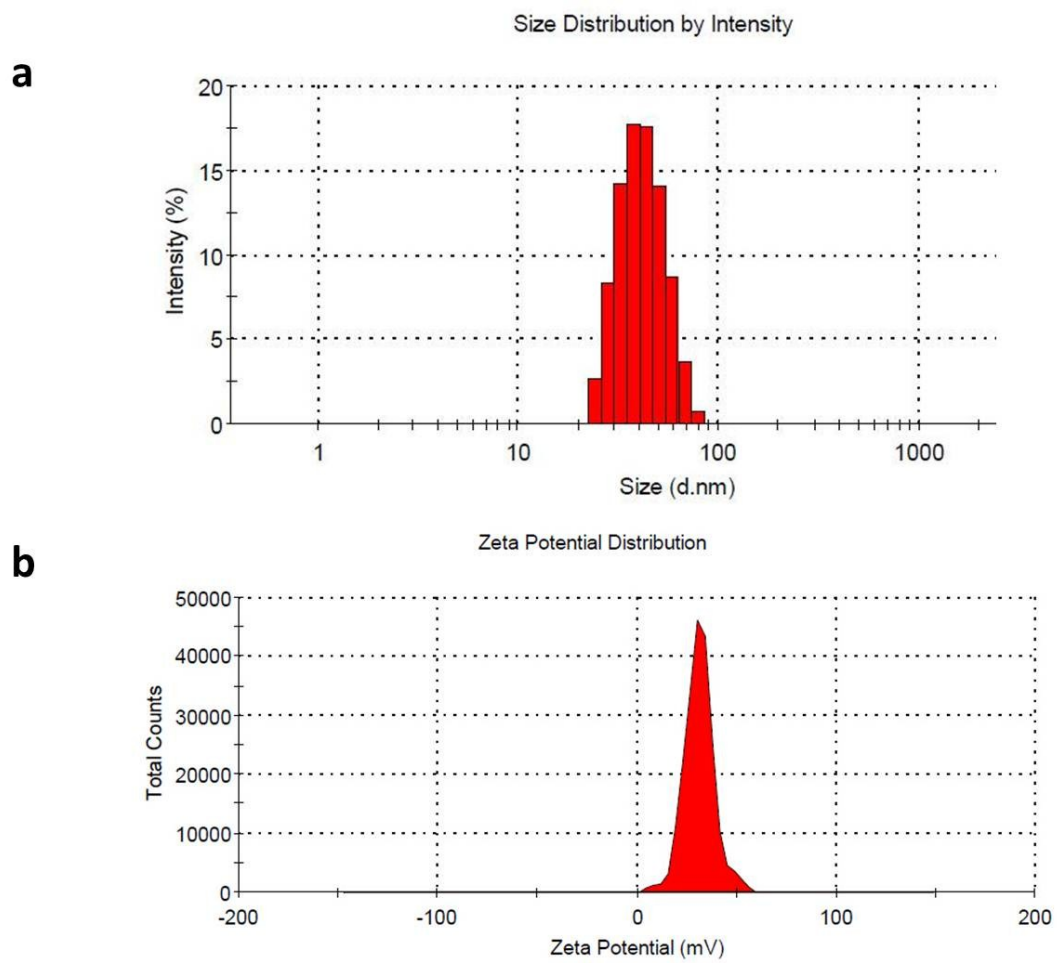


Fig. S3 Hydrodynamic size distribution (a) and Zeta potential (b) of Pt@BSA nanocrystals.

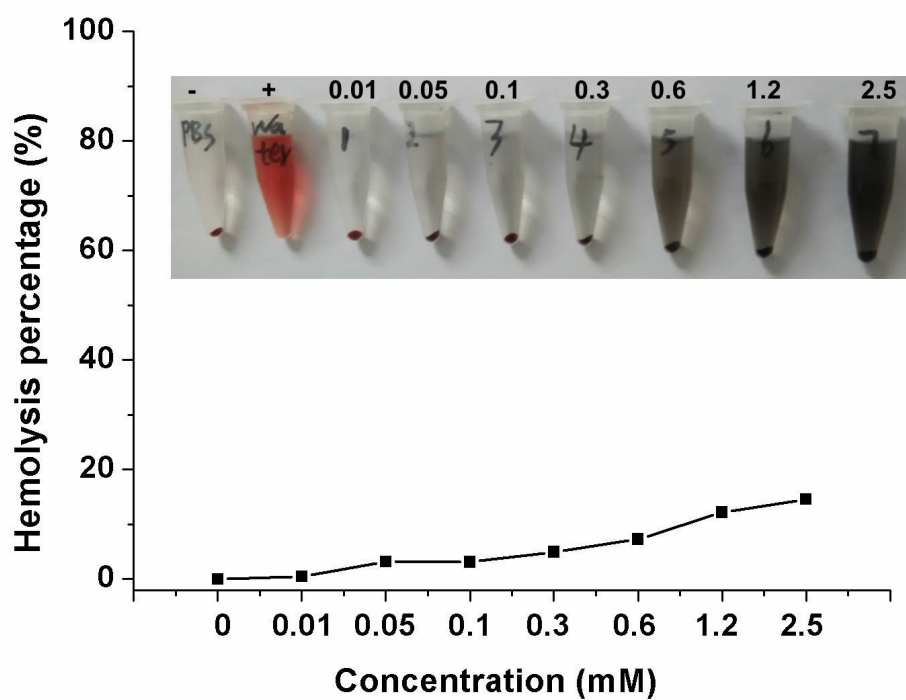


Fig. S4 Hemolysis percentage of the human red blood cells (HRBCs) suspensions after treated with different concentrations of Pt@BSA nanocrystals for 4 h using deionized water (+) and PBS (-) as positive and negative controls, respectively. Inset is the corresponding photographs for direct observing of hemolysis.

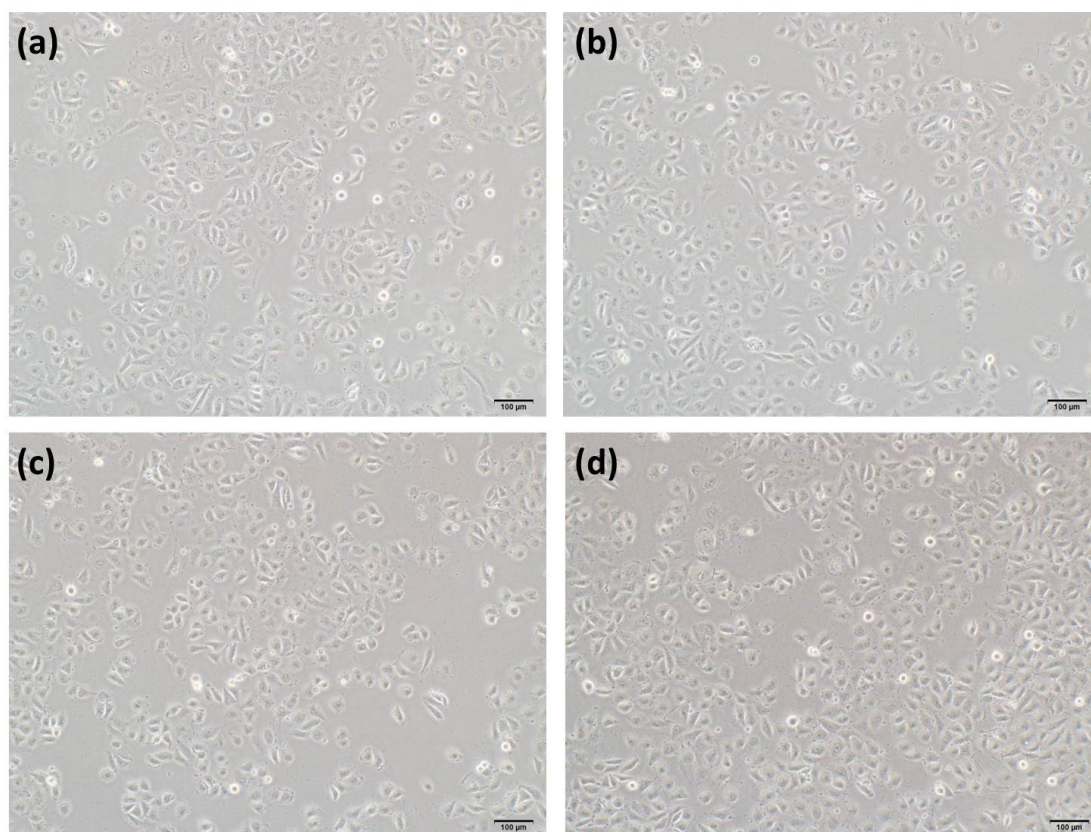


Fig. S5 Micrographs of A549 cells without treatment (a) and after treated with Pt@BSA nanocrystals at various platinum concentrations of 0.3 mM (b), 1.2 mM (c) and 2.5 mM (d) for 8 h.

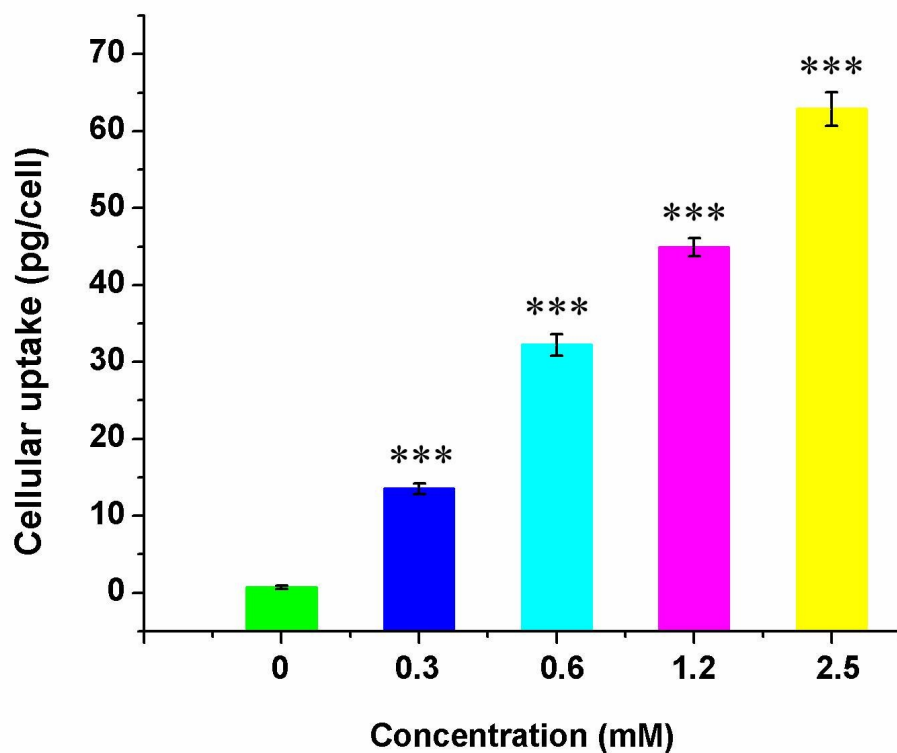


Fig. S6 ICP-OES analysis of platinum uptake by A549 cells after treated with different concentrations of Pt@BSA nanocrystals for 8 h. The statistical difference of platinum uptake by A549 cells after treated with Pt@BSA nanocrystals is in relative to the group without treatment (n=3, *P < 0.05, **P < 0.01 and ***P < 0.001).

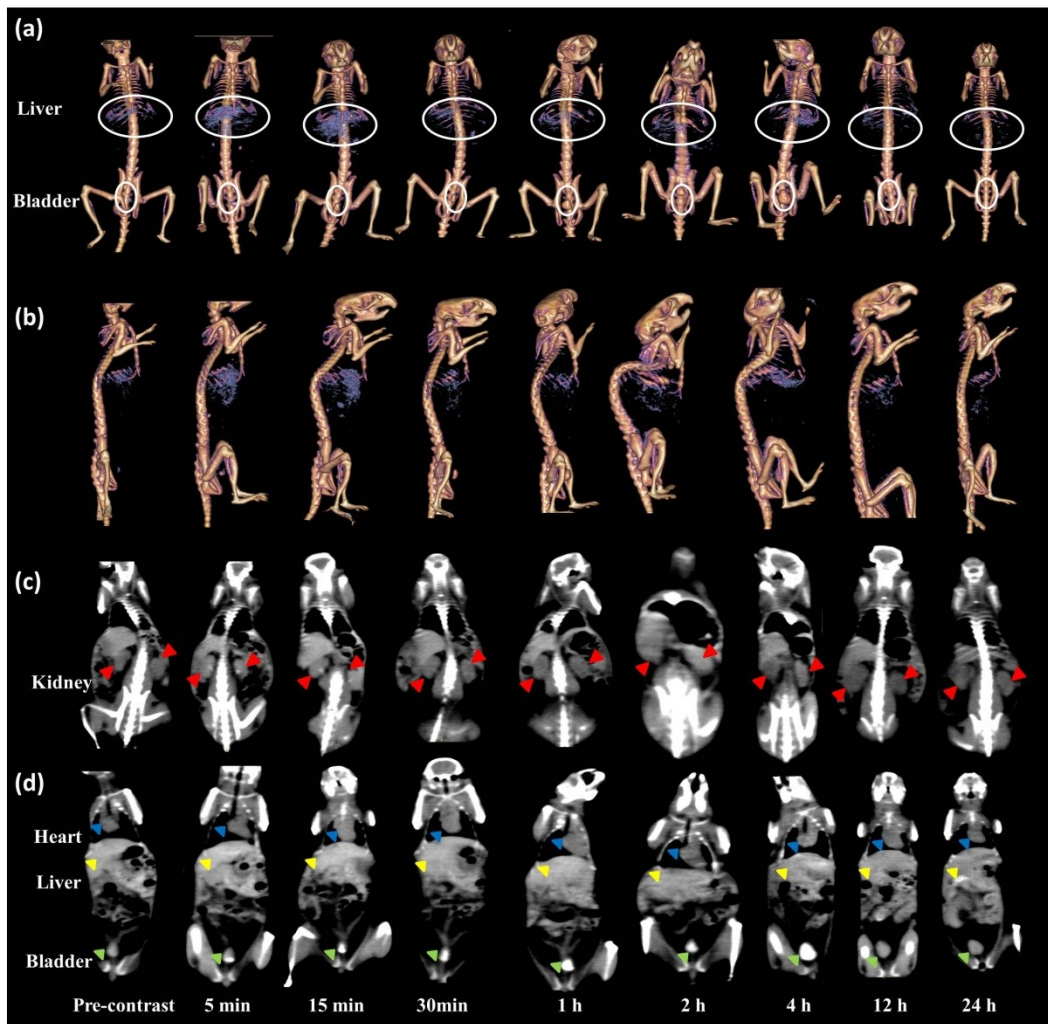


Fig. S7 CT images of a mouse in 3D rendering (a,b) and coronal views highlighted by kidney (c) and heart as well as liver and bladder (d) before and after intravenous injection of Ultravist with the equivalent molar dose comparing with Pt@BSA nanocrystals at various time intervals (red refers to kidney, blue refers to heart, yellow refers to liver and green refers to bladder).

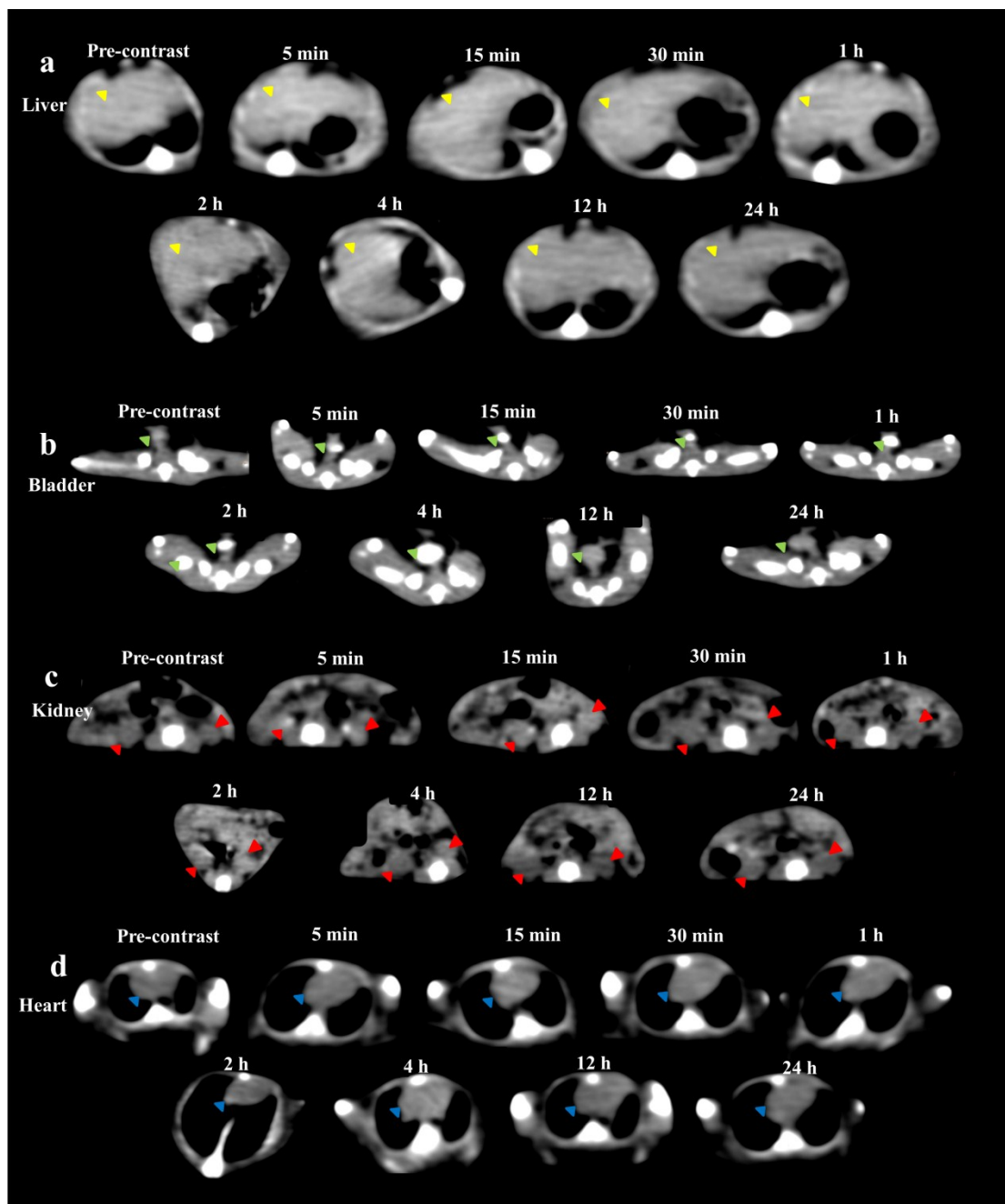


Fig. S8 CT images of a mouse liver (a), bladder (b), kidney (c) and heart (d) in transection before and after intravenous injection of Ultravist with the equivalent molar dose comparing with Pt@BSA nanocrystals at various time intervals (red refers to kidney, blue refers to heart, yellow refers to liver and green refers to bladder).

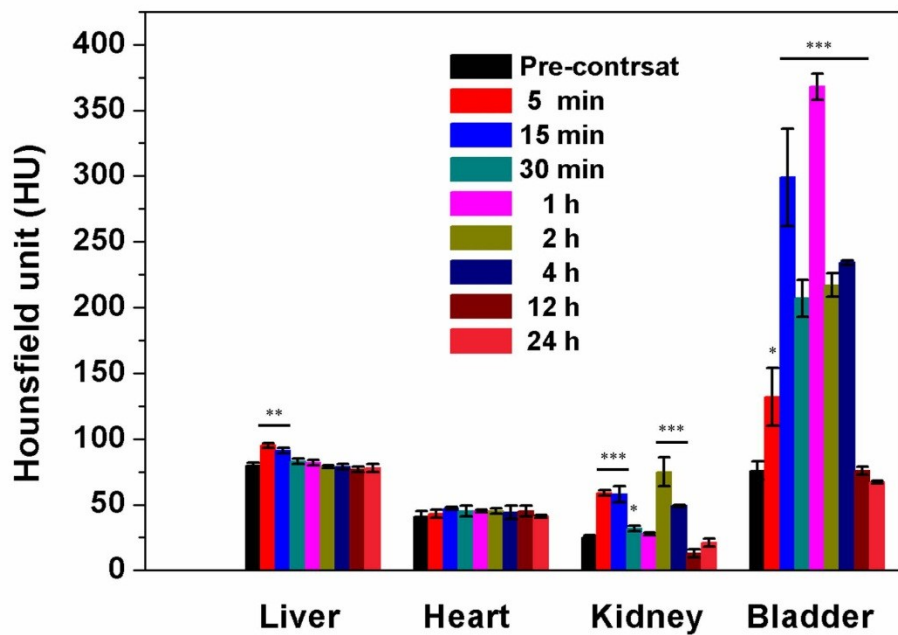


Fig. S9 CT values (HU) of different organs before after intravenous injection of Ultravist with the same molar concentration to Pt@BSA nanocrystals at various time intervals (n=3). All data are obtained in contrast to the mice prior to be injected with the agents (*P < 0.05, **P < 0.01 and ***P < 0.001).

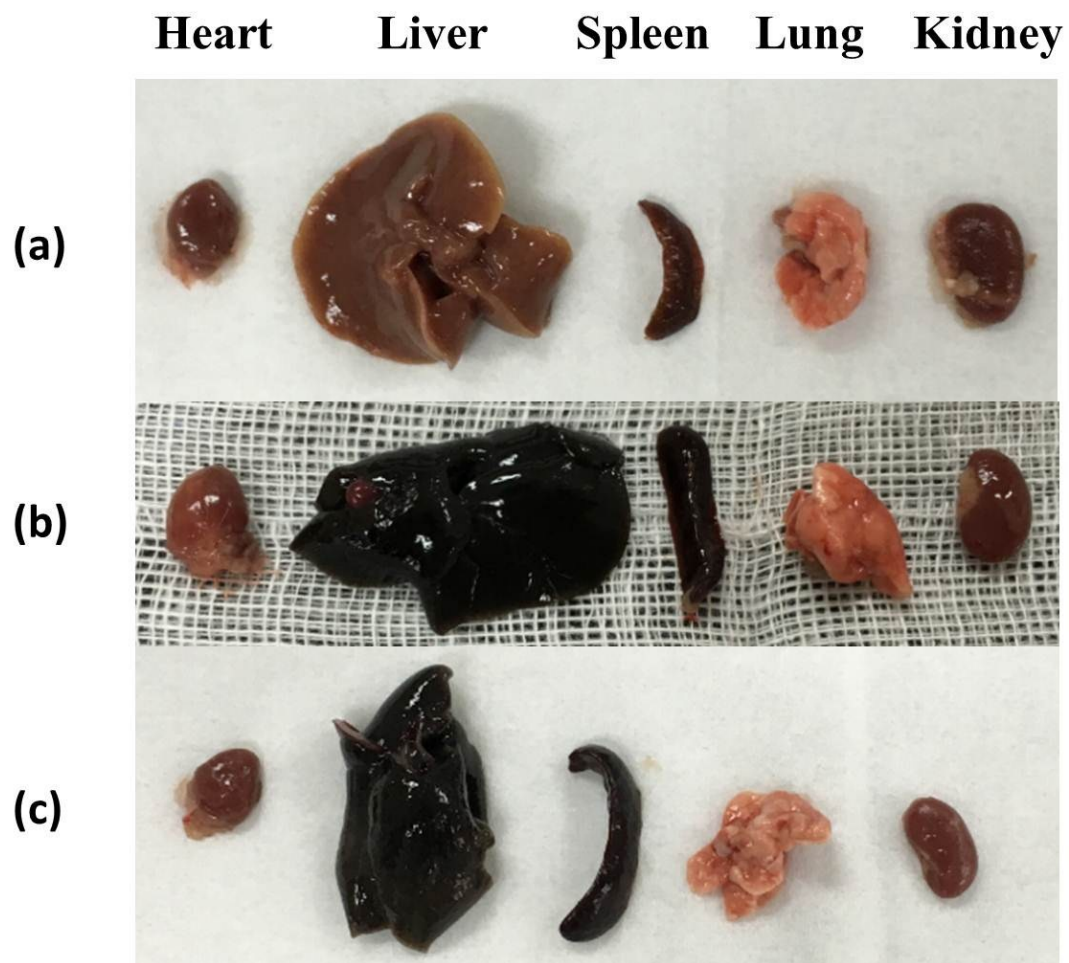


Fig. S10 Photographs of major organs including heart, liver, spleen, lung and kidney of the mice after intravenous injection of Pt@BSA nanocrystals ([Pt] = 10 mg/mL, 200 μ L in PBS) for 4 h (b) and 24 h (c), respectively. Mice injected with blank PBS (200 μ L) were served as comparisons (a).

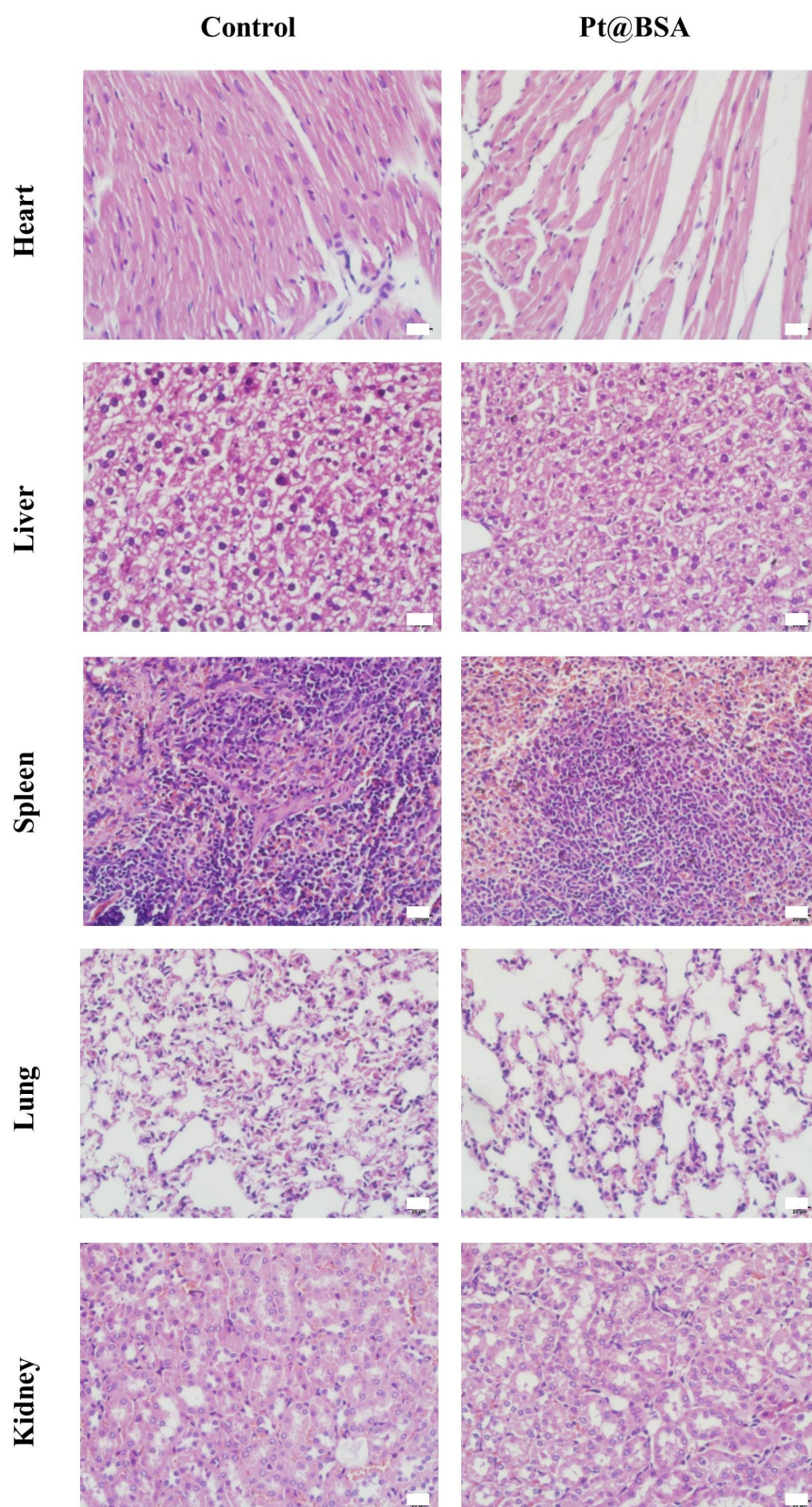


Fig. S11 H&E staining of major organs including heart, liver, spleen, lung and kidney of the mice after intravenous injection of Pt@BSA nanocrystals ([Pt] = 10 mg/mL, 200 μ L in PBS) for one week. Mice injected with PBS (200 μ L) were served as comparisons. The scale bar in each panel indicates 20 μ m (original magnification, $\times 40$, n = 3).